Chapter 8
Forest Fire Risk Zone Mapping in Tropical Forests of Saranda, Jharkhand, Using FAHP Technique

Sk Mujibar Rahaman, Masjuda Khatun, Sanjoy Garai, Pulakesh Das, and Sharad Tiwari

Abstract The forest fire has severe environmental and societal consequences causing millions of monetary losses every year in the form of loss of forest resources, animals, and man-made infrastructures globally. Mapping and monitoring of forest fire and its severity are essential to examine the loss of forest cover resources, environmental degradation, release of carbon, etc. The present study attempts to demarcate the forest fire-prone zones in Saranda forests, Jharkhand state, India, which houses Asia's largest Sal forest area (769 km^2). The Sentinel 2A multispectral satellite data and ALOS PALSAR digital elevation model (DEM) data were used to identify the forest-fire prone zones employing the fuzzy analytic hierarchy process (FAHP). The adopted method indicated a high modelling accuracy (overall 88% and kappa coefficient 84%). The study identified that about 77% area of the total forest area is under moderate to very high risk of a forest fire. The study suggests that the dense forest areas, which are characterized by high humidity and residing at higher altitudes, are less prone to a forest fire risk. Alternatively, the open and moderately dense forests at drier regimes are more prone to a forest fire. The developed maps are essential for forest cover management and preparedness to minimize the consequences of a forest fire. Various initiatives such as awareness programs, safeguarding forests from human interventions, formulation of forest fire task forces, and afforestation of native species in the open and disturbed forests in the moist areas are required to mitigate the forest fire risk in the Saranda forests.

Keywords Forest fire · FAHP · Sentinel 2A · ALOS PALSAR · Saranda forest

S. M. Rahaman · M. Khatun · S. Garai · S. Tiwari (✉)
Institute of Forest Productivity, Ranchi, Jharkhand, India
e-mail: tiwaris@icfre.org

P. Das
World Resource Institute, New Delhi, India
e-mail: pulakesh.das@wri.org

8.1   Introduction

The forest fire is described as uncontrolled burning of vegetation in a forested landscape. It is caused by various anthropogenic and natural factors including drought and warm climate and in some instances due to the occurrence of lightning (Taylor et al., 2008; Westerling et al., 2006). The climate-driven factors are the major causes of the forest fire, where the paleoclimatic studies have indicated higher fires accumulation during the prolonged drier period (Clark, 1988). The dry condition and heat waves have a direct influence on plant growth and humidity (Morgan et al., 2008). The increased dryness or drought condition due to climate alteration has significantly increased the fire events in the past few decades. Besides, the anthropogenic disturbances have induced changes in the land use/land cover (LULC) pattern, which is one of the prime reasons for increased forest fire (Running, 2006). The human interventions in the form of landscape development, land clearing for various purposes including agriculture or shifting cultivation in hilly terrains, and negligence during the tourism and other human activities are also regarded as causes of a forest fire (Behera et al., 2018).

The forest fire significantly contributes to the modification of the ecosystem structure. The fire severity determines the loss of vegetation cover and thereby the biodiversity and ecosystem productivity (Pausas, 2004; Piñol et al., 1998). Every year, fauna and flora in vast stretches of landscape are removed due to wildfire. It also has societal impacts via deteriorating human health and damages infrastructure. The forest fire releases enormous tree carbon into the atmosphere and significantly alters the regional to the global carbon budget (Spracklen et al., 2007). In the past few decades, several devastating forest fire instances have been reported globally such as Australian bush fire (2002, 06, 12, 13, 19–20), Russian wildfire (2003, 15), Northwest territories fires (2014), British Columbia wildfire (2017), Siberian wildfire (2019), Amazon rainforest wildfire (2019), California wildfire (2020), etc. (Iemima, 2018; Luke & McArthur, 2020; Pierce & Meyer, 2008)). In India, forest fire incidents are also frequent, where the recently reported incidences are Uttarakhand forest fire (2016) and Bandipur forest fire (2019) were the most devastating (Milton, 2019; Upadhyay, 2020).

Satellite remote sensing data provides a variety of indicators to assess the forest fire-driven changes in forest cover, structural attributes, biochemical properties, etc. The multitemporal analysis (i.e., pre- and post-fire images) allows to examine the changes in forest and land cover, wherein the GIS analysis facilitates the identification of drivers. Visual image interpretation of the satellite imagery allows the manual identification of fire burnt areas. Moreover, the changes in vegetation indices (spectral enhancement), e.g., Normalized Difference Vegetation Index (NDVI; normalized difference between near-infrared and red band) and Enhanced Vegetation Index (EVI; modified NDVI with canopy background soil correction factor) during the pre- and post-fire event, allow automatic identification. Several indices have been developed for effective burned area mapping, such as Normalized Burn Ratio (NBR; normalized difference between NIR and SWIR band), Normalized

Difference Moisture Index (NDMI); the pre- and post-event NBR (dNBR) and its relativized NBR (RdNBR) (Chuvieco et al., 2002; Key & Benson, 2005; Miller & Thode, 2007; Kolden et al., 2015). The Moderate Resolution Imaging Spectroradiometer (MODIS) and Medium Resolution Imaging Spectrometer (MERIS) sensor generate the global burnt area products at frequent intervals (1–3 days intervals) at a coarser resolution of 500 m and 30 m, respectively (Giglio et al., 2003; Alonso-Canas & Chuvieco, 2015), whereas the Landsat satellite data are widely used for forest fire mapping at moderate resolution (30 m) for the past five decades at various scales (Escuin et al., 2008; Long et al., 2019).

The forest fire occurrence maps created with the satellite data allows analyzing the causes of fire events integrating several response variables and proxies in the Geographical Information System (GIS) environment. The geospatial approach is recognized as a reliable method in developing fire susceptibility map in India, where a large portion of forest land is being occupied and managed by the forest dwellers (Jain et al., 1996; Roy et al., 1991). The statistical analysis of the past events and drivers enables examining the relative influence of the causative factors and allows to create a fire risk zone map (Chuvieco et al., 2010; Núñez-Regueira et al., 2000). Previous studies have identified several factors as biologic, physiographic, and anthropogenic. The biologic factors have significant impacts on forest fire incidence, where the forest fires have differential interactions depending on the species diversity and forest type (Kodandapani et al., 2008). Land use/land cover (LULC), vegetation density, and moisture content of vegetation determine the burnable fuel for forest fire expansion and severity (Biranvand et al., 2011; Adab et al., 2013; Siachalou et al., 2009). The moisture condition of vegetation plays a very influential factor in the spread of forest fire, where high moisturized areas are less prone to burning and vice-versa (Siachalou et al., 2009). The indices on vegetation greenness and moisture content as NDVI and NDMI, respectively, are widely used as the satellite data derived proxies (Serrano et al., 2000). Thin layers of a canopy with a higher reflectance in a short-wave infrared (SWIR) band signifies high moisture content, whereas the higher reflectance in NIR band indicates lower moisture content (Siachalou et al., 2009).

The physiographic variables as elevation and slope are linked with the wind and direction that act as stimulating factors and regulates the fire spread (Gao et al., 2011; Jaiswal et al., 2002; Weise & Biging, 1997). The downward spread of forest fire is slow as compared to the spread of intensity toward a higher slope (Kushla & Ripple, 1997). The moisture content determined by the amount of incident solar energy in an area is correlated with the aspect. The sun-facing aspects create favorable condition for the higher rate of fire spread owing to higher sunlight, heat, low clamminess, low fuel vapors, and heavy winds (Anderson, 1982; Prasad et al., 2008). The anthropogenic influences encourage the fire spread rate due to closeness to settlements and roads (Avila-Flores et al., 2010). Fire risk is higher as it offers more chance for unpredicted human-made explosions, due to the more forceful human actions (Alencar et al., 2004).

Jaiswal et al. (2002) employed the LISS-III data derived from forest type, slope, settlement, and road network map to map the forest fire risk zone in Gorna

Subwatershed, Madhya Pradesh, India. They have observed the high and very high risk in around 30% area of the total forest area. Kumari and Pandey (2020) integrated several factors such as fuel type, bare soil index, slope, aspect, elevation, distance from road, and settlement using the AHP technique for forest fire risk analysis in Palamau Tiger Reserve Forest, Jharkhand. They have observed a good agreement comparing with the MODIS and SNPP-VIRRS product and identified the high and very high-risk zone in about 43% of the area. Sharma et al. (2012) applied the Crisp AHP (CAHP) and Fuzzy AHP (FAHP) techniques for forest fire risk mapping in the Taradevi forest range of the Shimla Forest Division, India. The resultant map showed high accuracy with the forest fire observed data points and identified about 6.89 and 9% area as the very high-risk zone for the CAHP and FAHP technique, respectively. Kayet et al. (2020) compared the Frequency Ratio (FR) model and AHP technique for the forest fire risk mapping in Melghat Tiger Reserve forest, India. The validation with the Forest Survey of India (FSI) fire occurrence point data indicated an overall accuracy of 81% and 79% for the FR and AHP technique, respectively. Adab et al. (2013) employed the MODIS data product to compare the accuracies observed for various methods as Hybrid Fire Index, Structural Fire Index, and Fire Risk Index for northeast Iran. The receiver operating characteristic (ROC) curve indicated high accuracy of 76.7% for the hybrid fire index. Ahmad and Goparaju (2017) analyzed the forest fire hotspot districts in Jharkhand state, India, from 2005 to 2016 and reported the Paschim Singhbhum district as the most forest fire affected district.

In the present study, we have attempted to assess the forest fire risk in the Saranda Forest Division of Jharkhand using Fuzzy Analytic Hierarchy Process (FAHP) model and GIS. The objective of the study was to study the factors responsible for a forest fire in the Saranda Forest Division and to create a knowledge base that would enable better planning and management strategies to combat the future forest fire risk.

8.2   Study Area

The present study was conducted in the Saranda Forest Division (SFD) of West Singhbhum district, Jharkhand, India (Fig. 8.1). Saranda means "Land of Seven hundred Hills." It is Asia's largest dense Sal (*Shorea robusta*) forest and lies between 22° 22′ 58.83″ N to 22° 0′ 36.62″ N and 84° 58′ 47.35″ E to 85° 25′ 38.22″ E geographic extent and spread over about 1003 km² of geographical area. Jharkhand has about 29% of its geographical area under forest cover. Both protected forests (61%) and reserved forests (19%) are common to forest fires (Mishra, 2013). Previous studies have identified significant changes in forest cover in the Saranda Forest Division from 1992 to 2014 and built-up and mining area expansion replacing the dense and open forests. About 9% forest reduction with equivalent mining and built-up area expansion was reported by Kayet and Pathak (2015). The analysis
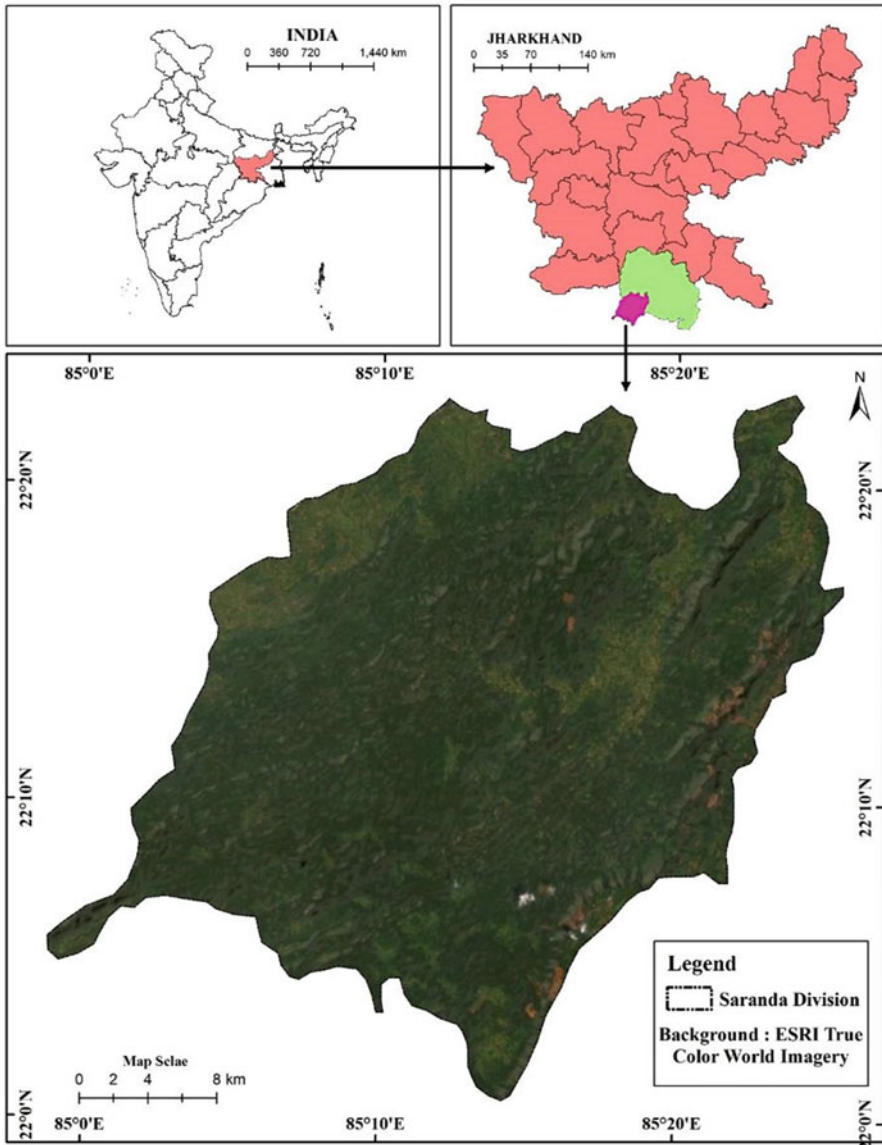
Fig. 8.1 Location map of the study area

carried out by the FSI (Forest Survey of India, 2019) estimated about 0.21%, 2.18%, and 9.16% area of Jharkhand falls under the extreme, very high, and highly fire-prone zones of the total forest cover in Jharkhand state.

8.3   Material and Methodology

Biologic Data

The biologic factors were introduced employing the NDVI and NDMI maps. These maps were prepared using the cloud-free Sentinel-2B level 2 high-resolution (10 m spatial resolution) satellite imagery dated March 28, 2020. The image tiles were accessed from the open-source archive of Copernicus Open Access Hub (https://scihub.copernicus.eu/).

Physiographic Data

The physiographic factors, i.e., elevation, slope, and aspect, were extracted from high resolution (12.5 mspatial resolution) ALOS PALSAR Digital Elevation Model (DEM) datasets acquired from National Aeronautics and Space Administration (NASA) Earth Observing Systems Data and Information Systems (EOSDIS) portal (https://search.asf.alaska.edu/#/?dataset=ALOS).

Anthropogenic Data

Proximity to road and settlement is sensitive factor for mapping forest fire risk zones. In the present study, road and settlement maps were prepared using Survey of India (SOI) 1:50k topographical map (73F3, 73F4, 73F7, 73F8, and 73B16) acquired from the data portal (https://soinakshe.uk.gov.in/).

Methodology

The various input layers were integrated, employing the AHP technique based on their relative importance.

The NDVI and NDMI maps were prepared using the QGIS 3.14 software employing the following formulae (Eqs. 8.1 and 8.2, respectively).

$$\text{NDVI} = \frac{\text{NIR} - \text{RED}}{\text{NIR} + \text{RED}} \tag{8.1}$$

$$\text{NDMI} = \frac{\text{NIR} - \text{SWIR}}{\text{NIR} + \text{SWIR}} \tag{8.2}$$

The NDVI layer was used to create the map vegetation and non-vegetation cover, where the NDVI threshold of 0.2 was considered for segregation (Al-doski, 2013). The leaf water content of the vegetation was assessed by the NDMI. Lower NDMI value indicates dry vegetation which is more flammable than fresh vegetation that has high NDMI value. Thus, alternative lower and higher weights were assigned to higher and lower moisture conditions areas.

The physiographic factors as elevation, slope, and aspect were derived from the ALOS DEM datasets using QGIS 3.14 software "raster terrain analysis" tool. Forest fire influences are higher in the lower altitude due to favorable climatic conditions; therefore, higher weightage was assigned to lower elevation (Jaiswal et al., 2002). The higher vertical slope increases the likelihood of increasing the spread of forest fires due to water loss and more efficient convection prewarming (Kushla & Ripple, 1997). Consequently, high and low slopes were assigned high and low weights, respectively. In the northern hemisphere, the south and the north-facing slope is exposed to highest and least sunlight, respectively, thus assigned contrasting higher and lower weightage (Kumari & Pandey, 2020).

Anthropogenic factors like distance from road and settlement were digitized from SOI topographical map on 1:50k scale. In the forest fire risk index, roads play both positive and negative roles. Roads offer more human access to forested areas enabling more human interference and increased chances of a spark of fire; alternatively, the roads create a barrier that prevents fire spreading. Areas close to the settlements and roads were assigned with higher weightage values. All the input variables were converted into raster format with uniform cell size and were projected for further processing.

Fuzzy Analytical Hierarchy Process (FAHP) Model

The FAHP is the combination of Analytic Hierarchy Process (AHP) and fuzzy logic. It follows a similar process to the AHP method. In FAHP, the arrays of the AHP are scaled into the fuzzy triangle scale to retrieve the importance of the input variables (Putra et al., 2018). Using a fuzzy triangle scale, fuzzified pairwise comparison matrix was prepared, as shown in Table 8.2.

Estimation of Geometric Mean

For each criterion, the geometric mean ($\widetilde{r_i}$) fuzzy comparison values are calculated as shown in the Eq. (8.3) (Buckley, 1985).

$$\widetilde{r_i} = \left(\prod_{j=1}^{n} \widetilde{d_{ij}} \right)^{\frac{1}{n}}, \quad i = 1, 2, 3, \ldots, n \tag{8.3}$$

Estimate Weight ($\widetilde{w_i}$):

$$\widetilde{w}_i = \widetilde{r}_i \bigotimes \left(\widetilde{r}_1 \bigotimes \widetilde{r}_2 \bigotimes \cdots \bigotimes \widetilde{r}_n \right)^{-1} \qquad (8.4)$$

Defuzzified (M_i):

$$M_i = \left(\frac{lw_i + mw_i + uw_i}{3} \right) \qquad (8.5)$$

Normalized Fuzzy Weight(N_i):

$$N_i = \frac{M_i}{\sum_{i-1}^{n} M_i} \qquad (8.6)$$

Forest Fire Risk Index

The input parameters as NDVI, NDMI, elevation, slope, aspect, distance to road, and distance to settlement were assigned different weights ranging from 2 to 10 based on their comparative importance to fire risk (Table 8.1). Lower and higher weightage value indicates the relative lower and higher hazard induced by the drivers. The mathematical equation used for calculating the forest fire risk index is shown below:

$$\begin{aligned} FFRI = &(V_m * 38) + (V_i * 20) + (e * 3) + (S * 14) + (a * 4) + (R * 12) \\ &+ (s * 10) \end{aligned} \qquad (8.7)$$

Where V_m is Normalised Difference Moisture Index, V_i is Normalised Difference Vegetation Index, e is elevation, S is slope, a is aspect, R is distance from road, s is distance to settlement, and 38, 20, 3, 14, 4, 12, 10 is the weight of the factor estimated by using the FAHP model (Tables 8.2, 8.3, and 8.4 and Eqs. 8.3–8.6).

For validation, the Suomi NPP and Visible Infrared Imaging Radiometer (SNPP-VIRS) forest fire dataset were used. The data were acquired from the Level-1 and Atmosphere Archive and Distribution System (LAADS) Distributed Active Archive

Table 8.1 Weights assigned to each variable and classes for forest fire risk modelling

Variables	Classes	Rating of risk
NDMI (−1 to +1)	<0, 0–0.16, 0.16–0.26, 0.26–0.36, >0.36	10, 8, 6, 4, 2
NDVI (−1 to +1)	<0.2, >0.2	4, 10
Elevation (m)	<350, 350–550, >550	10, 6, 2
Slope (°)	<5, 5–10, 10–15, 15–20, >20	2, 4, 6, 8, 10
Aspect(°)	North, East, West, South	4, 6, 8, 10
Proximity to Road(m)	<500, 500–1000, 1000–1500, 1500–2000, >2000	10, 8, 6, 4, 2
Proximity to Settlement(m)	<500, 500–1000, 1000–1500, 1500–2000, >2000	10, 8, 6, 4, 2

Table 8.2 Fuzzified pair-wise comparison matrix

Criteria	NDMI	NDVI	Elevation	Slope	Aspect	Proximity to road	Proximity to settlement
NDMI	**1, 1, 1**	4, 5, 6	5, 6, 7	5, 6, 7	6, 7, 8	5, 6, 7	5, 6, 7
NDVI	$\frac{1}{6}, \frac{1}{5}, \frac{1}{4}$	**1, 1, 1**	5, 6, 7	3, 4, 5	5, 6, 7	3, 4, 5	3, 4, 5
Elevation	$\frac{1}{7}, \frac{1}{6}, \frac{1}{5}$	$\frac{1}{7}, \frac{1}{6}, \frac{1}{5}$	**1, 1, 1**	1, 2, 3	$\frac{1}{3}, \frac{1}{2}, 1$	$\frac{1}{7}, \frac{1}{6}, \frac{1}{5}$	$\frac{1}{7}, \frac{1}{6}, \frac{1}{5}$
Slope	$\frac{1}{7}, \frac{1}{6}, \frac{1}{5}$	$\frac{1}{5}, \frac{1}{4}, \frac{1}{3}$	$\frac{1}{3}, \frac{1}{2}, 1$	**1, 1, 1**	$\frac{1}{3}, \frac{1}{2}, 1$	$\frac{1}{6}, \frac{1}{5}, \frac{1}{4}$	$\frac{1}{6}, \frac{1}{5}, \frac{1}{4}$
Aspect	$\frac{1}{8}, \frac{1}{7}, \frac{1}{6}$	$\frac{1}{7}, \frac{1}{6}, \frac{1}{5}$	1, 2, 3	1, 2, 3	**1, 1, 1**	$\frac{1}{6}, \frac{1}{5}, \frac{1}{4}$	$\frac{1}{6}, \frac{1}{5}, \frac{1}{4}$
Proximity to road	$\frac{1}{7}, \frac{1}{6}, \frac{1}{5}$	$\frac{1}{5}, \frac{1}{4}, \frac{1}{3}$	5, 6, 7	4, 5, 6	4, 5, 6	**1, 1, 1**	1, 2, 3
Proximity to settlement	$\frac{1}{7}, \frac{1}{6}, \frac{1}{5}$	$\frac{1}{5}, \frac{1}{4}, \frac{1}{3}$	5, 6, 7	4, 5, 6	4, 5, 6	$\frac{1}{3}, \frac{1}{2}, 1$	**1, 1, 1**

Table 8.3 Estimated geometric mean

Criteria	Geometric mean ($\widetilde{r}_i$)
NDMI	3.95, 4.63, 5.29
NDVI	1.96, 2.40, 2.85
Elevation	0.28, 0.36, 0.47
Slope	1.42, 1.67, 2.10
Aspect	0.34, 0.45, 0.57
Proximity to road	1.13, 1.43, 1.75
Proximity to settlement	0.96, 1.18, 1.50
Total (T)	10.04, 12.12, 14.52
Reverse (T^{-1})	0.10, 0.08, 0.07

Table 8.4 Estimated fuzzy weight

Criteria	Fuzzy weight ($\widetilde{w}_i$)	Defuzzified (M_i)	Normalized fuzzy weight (N_i)
NDMI	0.27, 0.38, 0.53	0.39	0.38
NDVI	0.14, 0.20, 0.28	0.21	0.20
Elevation	0.02, 0.03, 0.05	0.03	0.03
Slope	0.10, 0.14, 0.21	0.15	0.14
Aspect	0.02, 0.04, 0.06	0.04	0.04
Proximity to road	0.08, 0.12, 0.17	0.12	0.12
Proximity to settlement	0.07, 0.10, 0.15	0.10	0.10

Center (DAAC) website (https://ladsweb.modaps.eosdis.nasa.gov/). For validation, 222 points were created randomly, where the respective values were extracted from the forest fire risk map and SNPP-VIRS to compute the frequency and confusion matrix.

8.4   Result

The forest density map is shown in Fig. 8.2, which indicates the dominant occurrence of moderately dense forest (519 km^2) followed by open forest (281 km^2), grassland (83.65%), and dense forest (35.92%), whereas non-forest areas are estimated in 17.13 km^2 area. The factor maps are shown in Fig. 8.2. The NDMI map indicated higher moisture content for the grassland-dominated regions, as observed in the eastern and western part of the study area (Fig. 8.3a). The NDVI index map indicates the dominance of densely vegetated areas except for the eastern and northwestern part mostly occupied by grassland, settlement, and mining areas (Fig. 8.3b), which are also mostly in the lower altitudes (Fig. 8.3c). The corresponding slope map indicates lower slope in these regions and a higher slope in the rest of the study area (Fig. 8.3d). The aspect map indicates the face of the slope (Fig. 8.3e), which is categorized in four types as east, west, north, and south. The south-facing slope is given a higher value, and the north-facing slope is given a
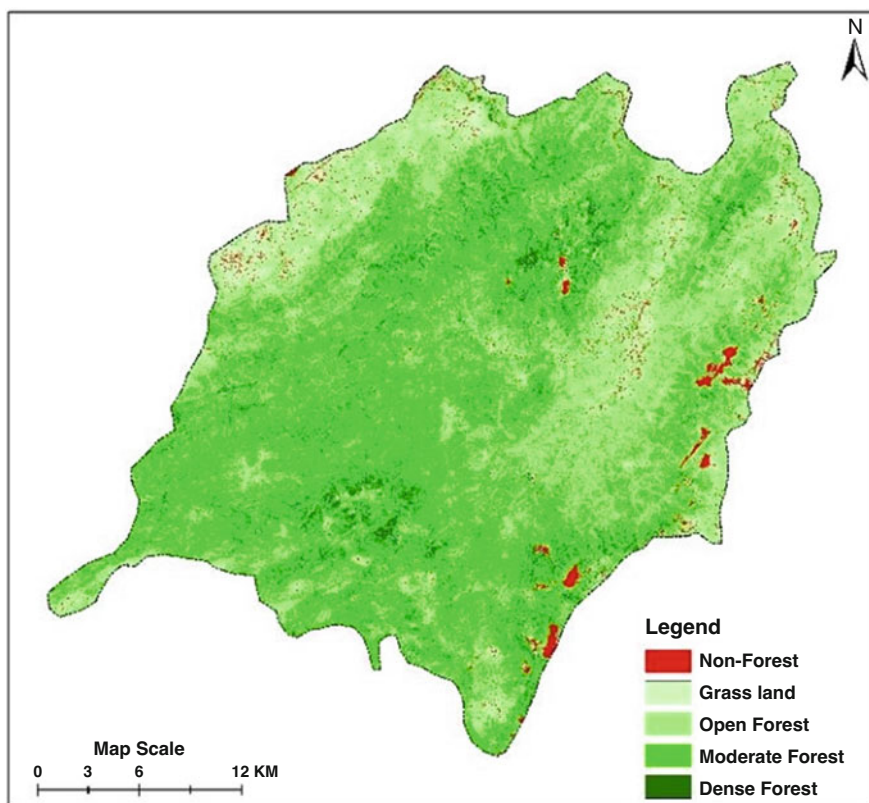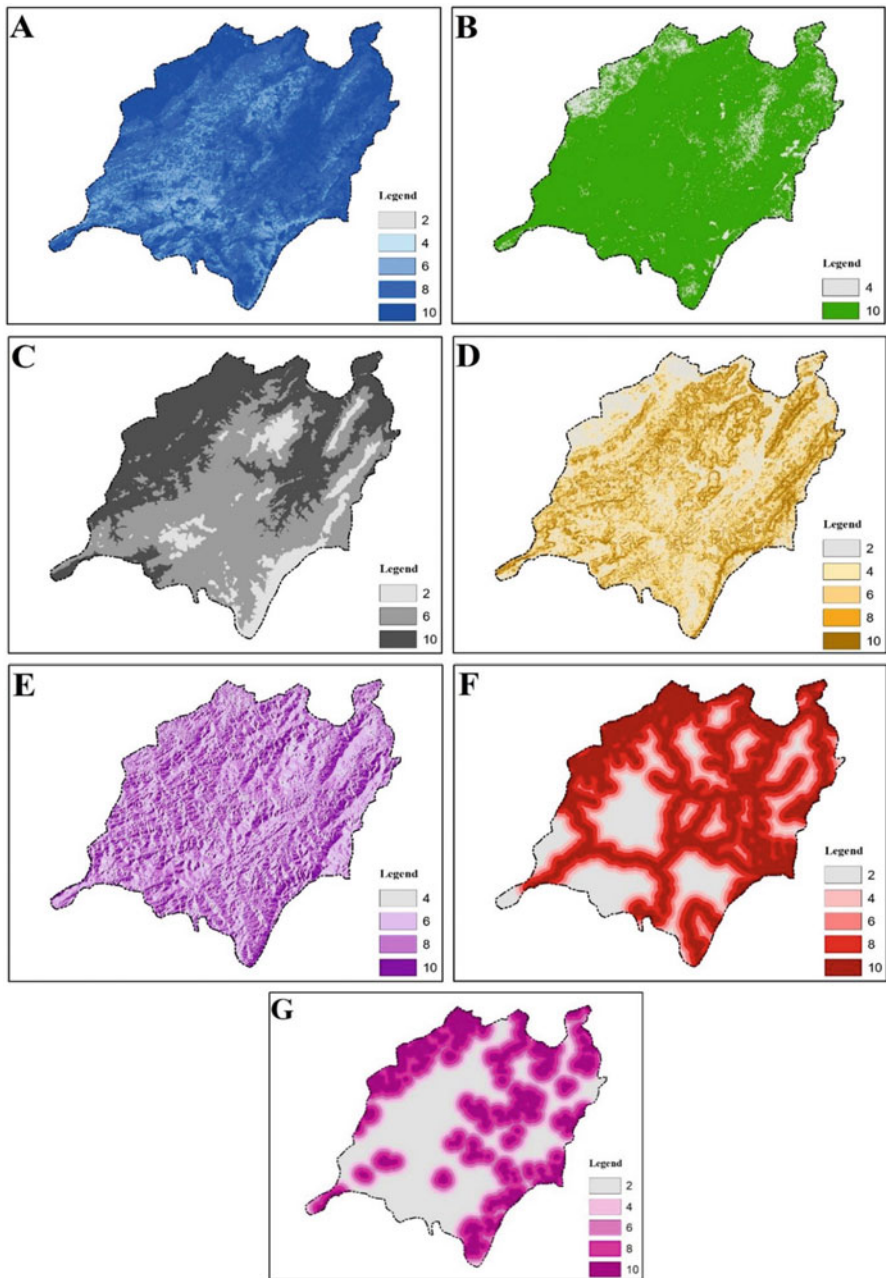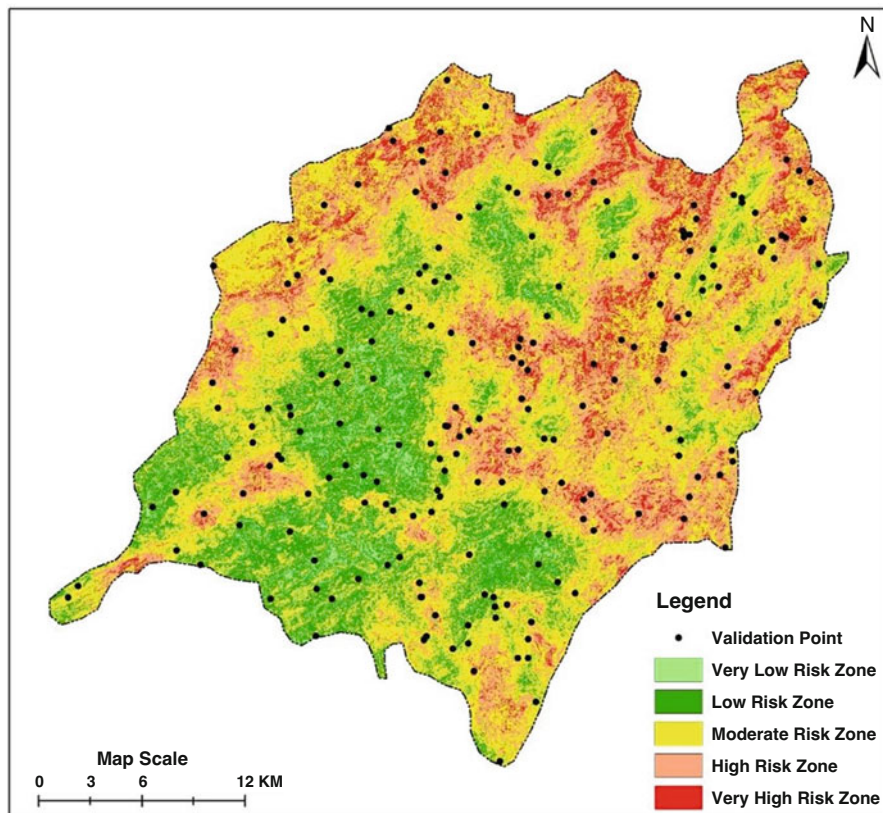

Fig. 8.2 Forest cover map

Fig. 8.3 Maps depicting: (**a**) Moisture Index, (**b**) Vegetation Index, (**c**) Elevation, (**d**) Slope, (**e**) Aspect, (**f**) Proximity to Road, and (**g**) Proximity to Settlement

Fig. 8.4 Forest Fire Risk Index map with validated points

lower value. The distance to road and settlement map are categorized into five groups, where the nearby places are given higher weightage and vice-versa.

The modelling accuracy is estimated comparing with the SNPP-VIRS forest fire data. The satellite data-derived forest fire points are overlaid on the derived forest fire risk zone map shown in Fig. 8.4. An error matrix is developed employing 222 random data points (Table 8.5). The lowest agreement is estimated for the very low-risk zone category, whereas high accuracy is observed for the rest of the categories. An overall accuracy of 88% is obtained with a kappa coefficient value of 0.84 (Table 8.6). The maximum producer's accuracy is observed the moderate- (98%) and high-risk (97%) zones categories followed by the low- (88%) and very high-risk (82%) zone.

The entire study area is classified into five risk zones, i.e., very high risk, high risk, moderate risk, low risk and very low risk. The area falling under different risk zones is calculated and is depicted in Table 8.7. Dominant forest covers in the eastern, northern, and western regions are estimated under moderate to high fire risk.

Table 8.5 Error matrix between the observed and predicted category

		Observed					
	Fire risk	Very low	Low	Moderate	High	Very high	Total
Predicted	Very low	8	1	0	0	0	9
	Low	2	37	1	0	0	40
	Moderate	4	1	88	0	1	94
	High	5	2	0	51	2	60
	Very high	2	2	0	2	13	19
	Total	21	43	89	53	16	222

Table 8.6 Error and accuracy estimate

Fire risk	Commission error	User accuracy	Omission error	Producer accuracy	Overall accuracy	Kappa value
Very low	11	89	24	76	88	84
Low	7	93	12	88		
Moderate	7	93	2	98		
High	15	85	3	97		
Very high	31	69	18	82		

Table 8.7 Area of forest fire risk zone

Risk zone	Area (km^2)	Percentage (%)
Very low	31.98	3.19
Low	201.38	20.07
Moderate	406.99	40.58
High	297.24	29.64
Very high	65.41	6.52

Alternatively, the forest covers in the low to very low-risk zones are mostly observed in the central and southern parts of the study area. The very high risk is estimated only 6.52% of the study area, whereas high- and moderate-risk zones are estimated in 29.64% and 40.58% area. The low-risk zone is estimated in 20.07%, whereas 3.9% area is estimated under the very low risk. The outcome of the study suggested that higher risk are mostly found in low-lying plain areas characterized by very low humidity, high slopes, ascending south, close to roads, and settlements. In contrast, areas characterized by high humidity, lesser land slope, and undisturbed forests are comparatively less prone to the occurrence and spread of forest fire.

Very-high fire risk is observed for open and moderately dense forests due to suitable biological, anthropogenic, and topographical conditions like less soil and vegetation moisture condition, gentle slope condition, low elevation, proximity to roads and settlements, and south-facing slope. In contrast, dense forests due to less human interference and its distribution along high altitudes fall under the low-risk zone. The moderately and open forest occupied the majority of the study area followed grassland, dense forest, and non-forest areas. In the dense forest, the
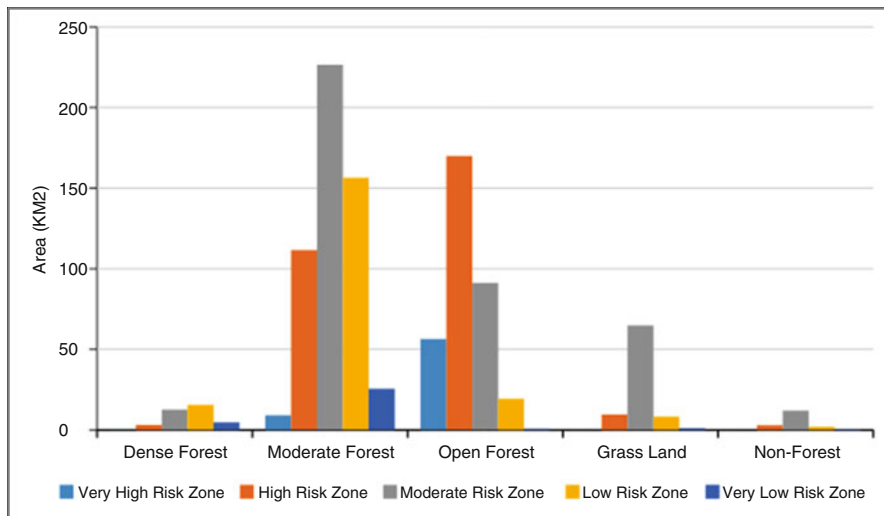
Fig. 8.5 Graph showing forest cover wise forest fire risk zone

majority of the area is estimated in lower-risk zone followed by moderate risk. Out of the total moderately dense forest of 519.6 km^2, the moderate risk zone is estimated in 226.38 km^{2}area followed by the low- (156.34 km^2) and high-risk zone (111.67 km^2) (Fig. 8.5). In the open forest, more than 60% of the area is estimated in the high-risk zone, whereas 32% area is estimated in the moderate risk-zone. The majority of areas under grassland are estimated in the moderate-risk zone (56.31 km^2) followed by nearly 5 km^2 and 4.5 km^2 under the high- and low-risk zones.

8.5   Discussion

Understanding the factors leading to an ecosystem vulnerable is important to assess ecosystem susceptibility (Chuvieco & Congalton, 1989). Almost 89% of the forest fires in tropical regions took place during the drier periods, e.g., March and April (Ahmad et al., 2018). West Singhbhum is the highest forest fire-prone district of Jharkhand state and experiences more than 30% of total forest fire of the state in about 17% of the state forest cover (Ahmad & Goparaju, 2017). The present study revealed that the open forests and moderate forest cover area form the majority forest cover, which is highly vulnerable to forest fire occurrence. Consequently, these parts are more dominated by human activities and experiencing an increase in surface temperature (Kayet et al., 2020). Human interventions could be one of the major drivers that ignite the forest fire (Dong et al., 2005). The study revealed that landscapes falling under the grassland category are prone to forest fire occurrence. The forest and grassland areas near the roads and settlements are more prone to fire

detonation because accidental fires can be caused by forest dweller and the tourists (Jaiswal et al., 2002). In comparison, the dense forests are estimated less prone to forest fire; which could be due to less human intervention and being distributed at a higher altitude. At higher altitudes, fire intensity remains less acute due to higher precipitation (Chuvieco & Congalton, 1989). Further, being densely distributed, the area is characterized by compactness, comparatively low temperature, and high moisture content, leading to a reduced risk of fire. Another major factor that contributes significantly to the spread of forest fire is wind. The densely distributed compact undisturbed forests act as a barrier to wind flow and thus reduce the forest fire intensity or spread. In contrast, moderately dense and open forest areas due to suitable biological, anthropogenic, and topographical conditions like low moisture, gentle slope, low elevation, open spaces, and proximity to roads and settlements provide an ideal environment for the occurrence of a forest fire. The Fuzzy AHP technique is successfully applied for the present study as indicated by the comparison (overall accuracy 88%) with the satellite-based observations. In comparison to FAHP, CAHP, and Dong model, FAHP and CAHP performed better (Sharma et al., 2012) than Dong model (Eskandari & Miesel, 2017). The study revealed that about ~23% area of Saranda forest falls under low- to very low-risk zone class and the remaining area ~77% that forms the majority of the Saranda forest division falls under moderate to very high risk prone zone and is vulnerable to forest fire incidents.

8.6 Control Measures

As the majority of the forest fire incidents are mostly caused by human activities, the prevention or control of forest fire can be achieved through people's participation. Identification and prioritization of the fire prone areas and region specific causes are more important. Creating awareness among local inhibitors living in the proximity of forests is very important. Various studies have suggested that the open and disturbed forest that are more prone to forest fire occurrence. These spaces shall be filled through afforestation programs based on the selection of native tree species supporting a high moisture environment. Formation of trained task forces equipped to deal with any situation of forest fire needs to be conformed and well-deployed in fields. Forest departments need to be equipped with modern firefighting equipment. Creation of small water resources like ponds and similar structures can be developed in the proximity of high-risk areas. Regular field monitoring, trained staff, and awareness among locals are some of the initiatives that can help to combat the forest fire.

8.7   Conclusion

The present study attempted to study the forest fire proneness in Saranda forests. The adopted methodology provided a reliable output well verified with the satellite-based observations. The study suggested that about 769 km^2 area of the study area, which is close to approximately ~77% of the total geographical area of Saranda forest division is vulnerable to moderate to very high risk of forest fire incidence. The various input maps and final forest risk zone map could be highly useful for the forest and biodiversity managers. The study exhibited that areas falling under vegetation class, i.e., grassland, open and moderately dense forests, are more prone to forest fire occurrence and dense forest areas are comparatively less prone to forest fire risk. The Saranda forest is one of the major Sal forests of Asia and is a hub to diverse species of economic and medicinal importance. Thus, the area needs special attention to safeguard it from increasing human interventions. Additionally, future studies may include assessment of the invasive species spread in the Saranda forests, as the presence of the bushy type of invasive weeds not only alter the native resources but also act as fire stimulation agents. An integrated approach in the form of research, awareness, and prioritization of area needs to be carried out to strengthen the management strategies to mitigate the increased risk of a forest fire.

References

Adab, H., Kanniah, K. D., & Solaimani, K. (2013). Modeling forest fire risk in the northeast of Iran using remote sensing and GIS techniques. *Natural Hazards, 65*(3), 1723–1743. https://doi.org/10.1007/s11069-012-0450-8

Ahmad, F., & Goparaju, L. (2017). Geospatial Assessment of Forest Fires in Jharkhand (India). *Indian Journal of Science and Technology, 10*(21), 1–7. https://doi.org/10.17485/ijst/2017/v10i21/113215

Ahmad, F., Uddin, M. M., & Goparaju, L. (2018). An evaluation of vegetation health and the socioeconomic dimension of the vulnerability of Jharkhand state of India in climate change scenarios and their likely impact: A geospatial approach. *Environmental and Socio-Economic Studies, 6*(4), 39–47. https://doi.org/10.2478/environ-2018-0026

Al-doski, J. (2013). NDVI differencing and post-classification to detect vegetation changes in Halabja City, Iraq. *IOSR Journal of Applied Geology and Geophysics, 1*(2), 01–10. https://doi.org/10.9790/0990-0120110

Alencar, A. A. C., Solórzano, L. A., & Nepstad, D. C. (2004). Modeling forest understory fires in an eastern amazonian landscape. *Ecological Applications, 14*(4 Suppl), 139–149. https://doi.org/10.1890/01-6029

Alonso-Canas, I., & Chuvieco, E. (2015). Global burned area mapping from ENVISAT-MERIS and MODIS active fire data. *Remote Sensing of Environment, 163*, 140–152. https://doi.org/10.1016/j.rse.2015.03.011

Anderson, H. E. (1982). *Aids to determining fuel models for estimating fire behavior* [Grass, shrub, timber, and slash, photographic examples, danger ratings]. In USDA Forest Service general technical report INT—Intermountain Forest and Range Experiment Station (USA).

Avila-Flores, D., Pompa-Garcia, M., Antonio-Nemiga, X., Rodriguez-Trejo, D. A., Vargas-Perez, E., & Santillan-Perez, J. (2010). Driving factors for forest fire occurrence in Durango State of

Mexico: A geospatial perspective. *Chinese Geographical Science, 20*(6), 491–497. https://doi.org/10.1007/s11769-010-0437-x

Behera, M. D., Gupta, A. K., Barik, S. K., Das, P., & Panda, R. M. (2018). Use of satellite remote sensing as a monitoring tool for land and water resources development activities in an Indian tropical site. *Environmental Monitoring and Assessment, 190*(7), 401.

Biranvand, A., Babaei, K. S., & Kiadaliri, H. (2011). *Investigation the ecological factors affecting fire spread in forest ecosystems (case study: Kakareza-Lorestan)*. USDA Forest Service General Technical Report INT-Intermountain Forest and Range Experiment Station (USA).

Buckley, J. J. (1985). Fuzzy hierarchical analysis. *Fuzzy Sets and Systems, 17*(3), 233–247. https://doi.org/10.1016/0165-0114(85)90090-9

Chuvieco, E., Aguado, I., Yebra, M., Nieto, H., Salas, J., Martín, M. P., Vilar, L., Martínez, J., Martín, S., Ibarra, P., de la Riva, J., Baeza, J., Rodríguez, F., Molina, J. R., Herrera, M. A., & Zamora, R. (2010). Development of a framework for fire risk assessment using remote sensing and geographic information system technologies. *Ecological Modelling, 221*(1), 46–58. https://doi.org/10.1016/j.ecolmodel.2008.11.017

Chuvieco, E., Martin, M. P., & Palacios, A. (2002). Assessment of different spectral indices in the red-near-infrared spectral domain for burned land discrimination. *International Journal of Remote Sensing, 23*(23), 5103–5110.

Chuvieco, E., & Congalton, R. G. (1989). 0034-4257-2889-2990023-0.Pdf. *Remote Sensing of Environment, 159*(29), 147–159.

Clark, J. S. (1988). Effect of climate change on fire regimes in northwestern Minnesota. *Nature, 334* (6179), 233–235.

Dong, X., Li-min, D., Guo-fan, S., Lei, T., & Hui, W. (2005). Forest fire risk zone mapping from satellite images and GIS for Baihe Forestry Bureau, Jilin, China. *Journal of Forestry Research, 16*(3), 169–174. https://doi.org/10.1007/bf02856809

Escuin, S., Navarro, R., & Fernández, P. (2008). Fire severity assessment by using NBR (Normalized Burn Ratio) and NDVI (Normalized Difference Vegetation Index) derived from LANDSAT TM/ETM images. *International Journal of Remote Sensing, 29*(4), 1053–1073. https://doi.org/10.1080/01431160701281072

Eskandari, S., & Miesel, J. R. (2017). Comparison of the fuzzy AHP method, the spatial correlation method, and the Dong model to predict the fire high-risk areas in Hyrcanian forests of Iran. *Geomatics, Natural Hazards and Risk, 8*(2), 933–949.

Forest Survey of India. (2019). India State of Forest Report (ISFR) 2019 (Issue 11.12 Jharkhand 11.12). Retrieved from https://fsi.nic.in/isfr19/vol2/isfr-2019-vol-ii-jharkhand.pdf

Gao, X., Fei, X., & Xie, H. (2011). Forest fire risk zone evaluation based on high spatial resolution RS image in Liangyungang Huaguo Mountain Scenic Spot. In *ICSDM 2011—Proceedings 2011 IEEE International Conference on Spatial Data Mining and Geographical Knowledge Services*, pp. 593–596. https://doi.org/10.1109/ICSDM.2011.5969116

Giglio, L., Descloitres, J., Justice, C. O., & Kaufman, Y. J. (2003). An enhanced contextual fire detection algorithm for MODIS. *Remote Sensing of Environment, 87*(2–3), 273–282.

Iemima, P. (2018). *Largest brush and forest fires in recorded history*. Worldatlas. Retrieved from https://www.worldatlas.com/articles/largest-brush-and-forest-fires-in-recorded-history.html

Jain, A., Ravan, S. A., Singh, R. K., Das, K. K., & Roy, P. S. (1996). Forest fire risk modelling using remote sensing and geographic information system. *Current Science*, 928–933.

Jaiswal, R. K., Mukherjee, S., Raju, K. D., & Saxena, R. (2002). Forest fire risk zone mapping from satellite imagery and GIS. *International Journal of Applied Earth Observation and Geoinformation, 4*(1), 1–10. https://doi.org/10.1016/S0303-2434(02)00006-5

Kayet, N., Chakrabarty, A., Pathak, K., Sahoo, S., Dutta, T., & Hatai, B. K. (2020). Comparative analysis of multi-criteria probabilistic FR and AHP models for forest fire risk (FFR) mapping in Melghat Tiger Reserve (MTR) forest. *Journal of Forestry Research, 31*(2), 565–579.

Kayet, N., & Pathak, K. (2015). Remote sensing and GIS based land use/land cover change detection mapping in Saranda Forest, Jharkhand, India. *International Journal of Earth Sciences, 3*(10), 1–6.

Key, C., & Benson, N. (2005). Landscape assessment: Ground measure of severity, the Composite Burn Index; and remote sensing of severity, the Normalized Burn Ratio. In *FIREMON: Fire effects monitoring and inventory system 2004*.

Kodandapani, N., Cochrane, M. A., & Sukumar, R. (2008). A comparative analysis of spatial, temporal, and ecological characteristics of forest fires in seasonally dry tropical ecosystems in the Western Ghats, India. *Forest Ecology and Management, 256*(4), 607–617. https://doi.org/10.1016/j.foreco.2008.05.006

Kolden, C. A., et al. (2015). Limitations and utilisation of Monitoring Trends in Burn Severity products for assessing wildfire severity in the USA. *International Journal of Wildland Fire, 24*(7), 1023–1028.

Kumari, B., & Pandey, A. C. (2020). Geo-informatics based multi-criteria decision analysis (MCDA) through analytic hierarchy process (AHP) for forest fire risk mapping in Palamau Tiger Reserve, Jharkhand state, India. *Journal of Earth System Science, 129*(1). https://doi.org/10.1007/s12040-020-01461-6

Kushla, J. D., & Ripple, W. J. (1997). The role of terrain in a fire mosaic of a temperate coniferous forest. *Forest Ecology and Management, 95*(2), 97–107. https://doi.org/10.1016/S0378-1127(97)82929-5

Long, T., Zhang, Z., He, G., Jiao, W., Tang, C., Wu, B., et al. (2019). 30 m resolution global annual burned area mapping based on Landsat Images and Google Earth Engine. *Remote Sensing, 11*(5), 489.

Luke, & McArthur (2020). Bushfire History, South Australian Country Fire Service. South Australian Country Fire Service. Retrieved from https://www.cfs.sa.gov.au/about-cfs/history-of-the-cfs/bushfire-history/

Miller, J. D., & Thode, A. E. (2007). Quantifying burn severity in a heterogeneous landscape with a relative version of the delta Normalized Burn Ratio (dNBR). *Remote Sensing of Environment, 109*(1), 66–80.

Milton, L. (2019). Karnataka: Bandipur fire doused, forest official confirms act of sabotage. *Times of India*. Retrieved from https://timesofindia.indiatimes.com/city/mysuru/karnataka-bandipur-fire-doused-forest-official-confirms-act-of-sabotage/articleshow/68145439.cms

Mishra, A. K. N. (2013). More forests burning in Jharkhand. *Times of India*. Retrieved from https://timesofindia.indiatimes.com/city/ranchi/More-forests-burning-in-Jharkhand/articleshow/19504839.cms?utm_source=contentofinterest&utm_medium=text&utm_campaign=cppst&pcode=461

Morgan, P., Heyerdahl, E. K., & Gibson, C. E. (2008). Multi-season climate synchronized forest fires throughout the 20th century, northern Rockies, USA. *Ecology, 89*(3), 717–728. https://doi.org/10.1890/06-2049.1

Núñez-Regueira, L., Proupín-Castiñeiras, J., & Rodríguez-Añón, J. A. (2000). Design of risk index maps as a tool to prevent forest fires in the hill-side zone of Galicia (NW Spain). *Bioresource Technology, 73*, 123–131.

Pausas, J. G. (2004). Peninsula (Mediterranean Basin). *Climatic Change, 63*, 337–350.

Pierce, J., & Meyer, G. (2008). Long-term fire history from alluvial fan sediments: The role of drought and climate variability, and implications for management of Rocky Mountain forests. *International Journal of Wildland Fire, 17*(1), 84–95.

Piñol, J., Terradas, J., & Lloret, F. (1998). Climate warming, wildfire hazard, and wildfire occurrence in coastal eastern Spain. *Climatic Change, 38*(3), 345–357. https://doi.org/10.1023/A:1005316632105

Prasad, V. K., Badarinath, K. V. S., & Eaturu, A. (2008). Biophysical and anthropogenic controls of forest fires in the Deccan plateau, India. *Journal of Environmental Management, 86*(1), 1–13. https://doi.org/10.1016/j.jenvman.2006.11.017

Putra, M. S. D., Andryana, S., & Fauziah, & Gunaryati, A. (2018). Fuzzy analytical hierarchy process method to determine the quality of gemstones. *Adv. Fuzzy Syst., 2018*. https://doi.org/10.1155/2018/9094380

Roy, P. S., Ranganath, B. K., Diwakar, P. G., Vohra, T. P. S., Bhan, S. K., Singh, I. J., & Pandian, V. C. (1991). Tropical forest typo mapping and monitoring using remote sensing. *International Journal of Remote Sensing, 12*(11), 2205–2225. https://doi.org/10.1080/01431169108955253

Running, S. W. (2006). Is global warming causing more, larger wildfires? *Science, 313*(5789), 927–928. https://doi.org/10.1126/science.1130370

Serrano, L., Ustin, S. L., Roberts, D. A., Gamon, J. A., & Peñuelas, J. (2000). Deriving water content of chaparral vegetation from AVIRIS data. *Remote Sensing of Environment, 74*(3), 570–581. https://doi.org/10.1016/S0034-4257(00)00147-4

Sharma, L. K., Kanga, S., Nathawat, M. S., Sinha, S., & Pandey, P. C. (2012). Fuzzy AHP for forest fire risk modeling. *Disaster Prevention and Management: An International Journal.*

Siachalou, S., Doxani, G., & Tsakiri-Strati, M. (2009). Integrating remote sensing processing and GIS to fire risk zone mapping: A case study for the Seih-Sou Forest of Thessaloniki. In *Proceedings of the 24th International Cartographic Conference (ICC), January 2016*, pp. 1–10. Retrieved from http://icaci.org/documents/ICC_proceedings/ICC2009/html/nonref/6_10.pdf

Spracklen, D. V., Logan, J. A., Mickley, L. J., Park, R. J., Yevich, R., Westerling, A. L., & Jaffe, D. A. (2007). Wildfires drive interannual variability of organic carbon aerosol in the western U.S. in summer. *Geophysical Research Letters, 34*(16), 2–5. https://doi.org/10.1029/2007GL030037

Taylor, A. H., Trouet, V., & Skinner, C. N. (2008). Climatic influences on fire regimes in montane forests of the southern Cascades, California, USA. *International Journal of Wildland Fire, 17*(1), 60–71. https://doi.org/10.1071/WF07033

Upadhyay, V. (2020). Second-worst in 16 yrs, fires destroy 2521 ha forest cover in Uttarakhand. *Times of India*. Retrieved from http://timesofindia.indiatimes.com/articleshow/69660263.cms?utm_source=contentofinterest&utm_medium=text&utm_campaign=cppst_prime

Weise, D. R., & Biging, G. S. (1997). A qualitative comparison of fire spread models incorporating wind and slope effects. *Forest Science, 43*(2), 170–180.

Westerling, A. L., Hidalgo, H. G., Cayan, D. R., & Swetnam, T. W. (2006). Warming and earlier spring increase Western U.S. forest wildfire activity. *Science, 313*(5789), 940–943. https://doi.org/10.1126/science.1128834